NMR evidence of the magnetic phase separation in $Pr_{0.5}Ca_{0.2}Sr_{0.3}MnO_3$ manganite

M. M. Savosta and A. S. Karnachev
Donetsk Institute of Physics & Technics, Academy of Sciences of Ukraine, Rozy Luxembourg 72, 83114 Donetsk, Ukraine

S. Krupička, J. Hejtmánek, Z. Jirák, M. Maryško, and P. Novák
Institute of Physics, Academy of Sciences of the Czech Republic, Na Slovance 2, 182 21 Praha 8, Czech Republic
(Received 5 January 2000)

The local ferromagnetism in $Pr_{0.5}Ca_{0.2}Sr_{0.3}MnO_3$ manganite was investigated by means of ^{55}Mn NMR for temperatures up to $T_C = 220$ K. Below the ferromagnetic to antiferromagnetic transition NMR detects a minority ferromagnetic phase, which gives rise to two NMR lines having comparable amplitudes. One of these lines is attributed to the volume, while the other to the boundary of the ferromagnetic microdomains. For $T \geqslant T_N$ another line corresponding to the bulk ferromagnetism appears, which coexists with the signal from the minority ferromagnetic phase. All NMR signals display conspicuous thermal hysteresis of the amplitude, reflecting the first-order character of the ferromagnetic $\leftrightarrow$ antiferromagnetic transition. In addition a hysteresis of the frequency of the minority ferromagnetic phase signal was also observed. The results demonstrate a specific case of the microscopic phase separation.

Manganite perovskites $R_{1-x}A_xMnO_3$ with $x = 0.5$ exhibit a rich phase diagram, connected with the competition of antiferromagnetic (AFM) superexchange, ferromagnetic (FM) double exchange, charge ordering, Jahn-Teller effect of Mn^{3+} ion, etc. For the same reason a strong tendency to the phase separation exists in these systems (see Ref. 1 for a recent survey). Using the high-resolution electron microscopy it was shown recently that the FM-AFM transition in $La_{0.5}Ca_{0.5}MnO_3$ is accompanied by a coexistence of incommensurate charge-ordered and ferromagnetic charge-disordered microdomains with a size of 20–30 nm.[2] Fukumoto *et al.*[3] found in $Nd_{0.5}Sr_{0.5}MnO_3$ that the transition process from the charge-ordered state to the FM one is characterized by the nucleation and growth of the FM metallic phase regions along the antiphase boundaries in the charge-ordered phase. On the other hand, NMR on ^{55}Mn in $Pr_{0.5}Sr_{0.5}MnO_3$ (Ref. 4) suggests that the low-temperature magnetic state consists of microscopic ferromagnetic domains with a very large surface to volume ratio, embedded in the AFM matrix. A number of papers on $La_{0.5}Ca_{0.5}MnO_3$ have appeared, in which the ^{139}La and ^{55}Mn NMR in was studied.[5–9] Most of the authors have observed complex, double-peaked line shape of spectra in the region of FM-AFM transition, the origin of which is far from being clear. Papavassiliou *et al.* in their recent paper[9] assigned these two peaks to FM metallic and FM insulating regions, respectively. Dho *et al.*[7] proposed two metallic FM phases, which are distinguished by density of mobile e_g electrons. Finally, in Ref. 8 two La sites experiencing different covalent configurations with respect to the nearest Mn ions, likely caused by the charge-orbital ordering, were detected.

In this paper we study the temperature dependence of ^{55}Mn NMR in $Pr_{0.5}Ca_{0.2}Sr_{0.3}MnO_3$ manganite. The properties of this material are very similar to those of $La_{0.5}Ca_{0.5}MnO_3$. In particular, the low-temperature state of two systems is the same, i.e., the CE-type antiferromagnetism dominates. In the present compound we have detected both the minority microscopic ferromagnetic regions at low temperatures and the bulk ferromagnetism at elevated temperatures. We show unambiguously that these two ferromagnetic phases are different in nature and they coexist in certain temperature interval. On cooling, $Pr_{0.5}Ca_{0.2}Sr_{0.3}MnO_3$ first undergoes a FM transition at 220 K, then follows a first-order transition to AFM state at $T_N \approx 160$ K (180 K on warming).[10] At temperatures above T_N comparatively large magnetic moment $\approx 1.5\mu_B$ per Mn ion is observed, corresponding to a macroscopic ferromagnetism. Residual magnetic moment $\approx 0.17\mu_B$ is observed at low temperatures. The present NMR results were collected on the same polycrystalline sample, prepared as described in Ref. 10, where the results of magnetization, transport measurements, and the neutron diffraction were given.

The NMR spectra were recorded by a two-pulse spin-echo method at temperatures between 77 and 220 K using a noncoherent spectrometer with frequency sweep and boxcar detector signal averaging. The length t of the pulses was 0.5 μs, the amplitude of the radiofrequency (rf) field for the optimal spin-echo excitation B_{rf}^{opt} was found to increase approximately from 1.5 to 2 G, as the temperature of measurement was raised. Besides, in the temperature interval 150–170 K B_{rf}^{opt} was found to change slightly through the NMR spectrum. The optimal value of the rf field was used to determine the enhancement factor η (see, for example, Ref. 11) for the ^{55}Mn nuclei, which contribute to the spin-echo signal at a given frequency:

$$\eta = \frac{1}{3t(\gamma/2\pi)B_{rf}^{opt}}, \tag{1}$$

where $\gamma/2\pi = 10.6$ MHz/T for ^{55}Mn. All the signals detected come from the ferromagnetic regions as follows from the characteristic high values of the enhancement factor $\eta \approx 300-400$. Besides, the signal from the antiferromagnetic regions relaxes too fast[4] to be observed at temperatures of our measurements. In order to take into account the effect of

 ©2000 The American Physical Society

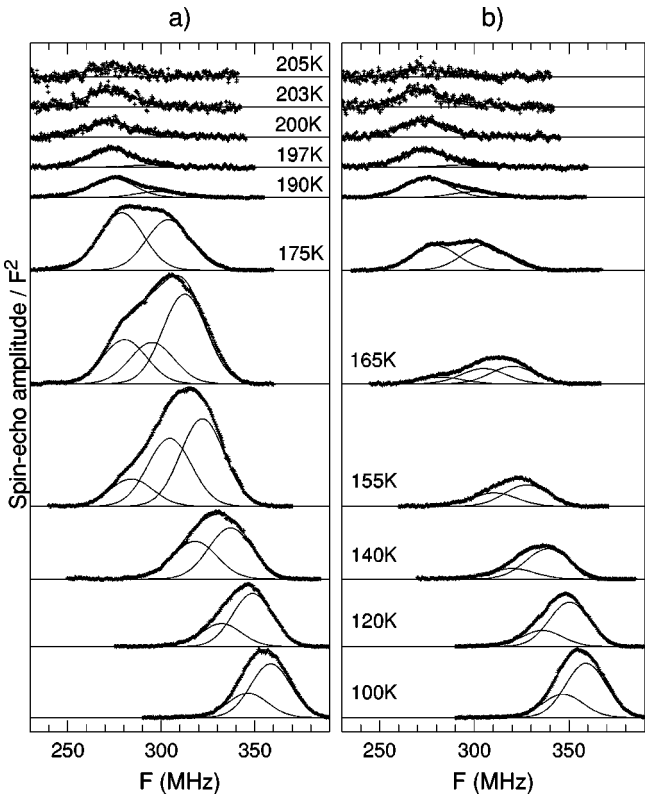

FIG. 1. The temperature dependence of ^{55}Mn NMR spectra in $Pr_{0.50}Ca_{0.20}Sr_{0.30}MnO_3$ taken at cooling (a) and warming (b). The spectra are decomposed into three lines (full curves) as described in the text.

the spin-spin nuclear relaxation on the NMR spectra, for each temperature the data were collected for several time intervals τ between the exciting and refocusing rf pulses, starting from $\tau_{min}=3\mu$s. Having in mind that the relaxation rate may depend on the rf power,[12] the excitation condition was kept constant throughout the spectrum.

The NMR spectra at selected temperatures, taken on cooling and warming for $\tau=3\mu$s are displayed in Fig. 1. The spectra are complex, their line shape depends on the temperature and they exhibit a clear thermal hysteresis. For the following discussion the temperature interval of the measurement is divided into three parts. At low temperatures ($T \leqslant 150$ K on cooling, 160 K on warming) the spectrum is decomposed in two Gaussian lines, which have similar amplitude, but different spin-spin relaxation time T_2. We arrived at this conclusion, because the form of the spectra exhibits a specific dependence on the time interval τ. As seen in Fig. 2, the width of the spectrum first decreases when increasing τ, then remains constant, however. The decrease of the width is accompanied by the frequency shift of the center of gravity of the spectrum. This behavior may be understood if the spectrum consists of the two lines A_1, A_2 having different NMR frequencies, the first line with slow , the second with fast spin-spin relaxation ($T_2^{A_1} > T_2^{A_2}$). For each line the intensity I of the spin echo is expected to be

$$I = I_0 \exp(-2\tau/T_2). \tag{2}$$

If $\tau \leqslant T_2^{A_1}, T_2^{A_2}$ is fulfilled, both lines contribute to the signal observed, while for long enough delay time ($\tau \gg T_2^{A_2}$) only

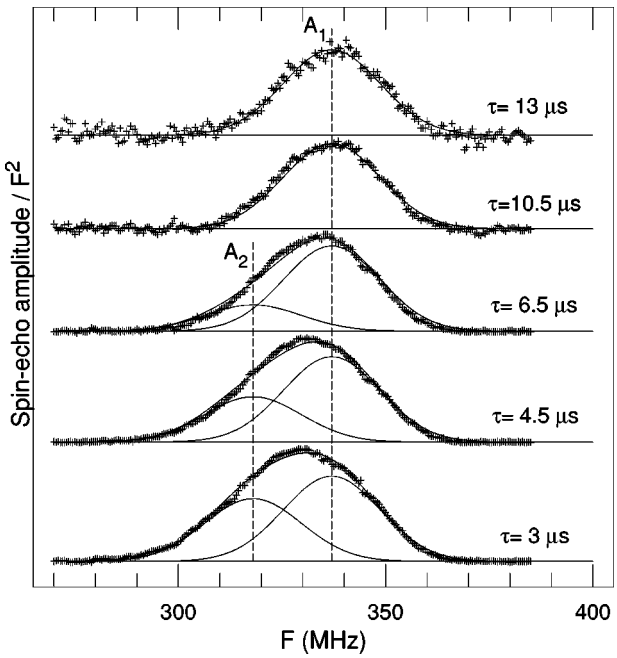

FIG. 2. NMR spectrum of ^{55}Mn at $T=140$ K (cooling) taken for different values of τ. Spectra for $\tau=4.5$, 6.5, 10.5, and 13μs are increased by factor 1.5, 2.3, 6.4 and 13, respectively. The spectra are decomposed into two lines A_1 and A_2 with fixed frequencies and linewidths.

the contribution of the slow relaxing line A_1 remains.

In the temperature interval 150–170 K the NMR spectrum qualitatively changes, as a new contribution (line B) gradually develops. The relaxation of the new line is still faster comparing to the relaxation of line A_2 and due to its pronounced thermal hysteresis the temperature at which it appears on warming ($T \approx 160$ K) differs markedly from the temperature at which it disappears on cooling ($T \approx 150$ K). Figure 3 shows the spectra taken at $T=155$ K for different time delay τ together with corresponding decomposition on two (warming) and three (cooling) lines, respectively.

Finally, for temperatures higher than ≈ 170 K the spectrum may be described as a superposition of the two lines B and A_1 only. The relative contribution of the B line gradually increases and for $T \geqslant 197$ K only the line B is detected.

Each of the lines A_1, A_2, B can be characterized by resonance frequency F, amplitude I_0, relaxation time T_2 and linewidth ΔF. We obtained these quantities by analyzing the NMR spectra taken at different time delays at each separate temperature. The analysis is made easier by the fact that the relaxation times of individual lines differ markedly, so that (with only a few exceptions) for long τ only line A_1 with the slowest relaxation survives. It is interesting to note that the linewidth obtained by the analysis is about the same for all three lines $\Delta F \approx 27.5$ MHz for $T \geqslant 140$ K and slightly decreases with decreasing temperature to $\Delta F \approx 25$ MHz ($T=77$ K). The temperature dependences of F and T_2 are shown in Fig. 4. Resonance frequency of the lines A_1 and A_2 exhibits a thermal hysteresis, while no such hysteresis was found for F of the line B. Temperature dependences of T_2 are different for different lines. A small thermal hysteresis of this dependence was found for line A_2 only. $T_2^{-1}(T)$ of line A_1 has an exponential form, similar to the one found by us in the

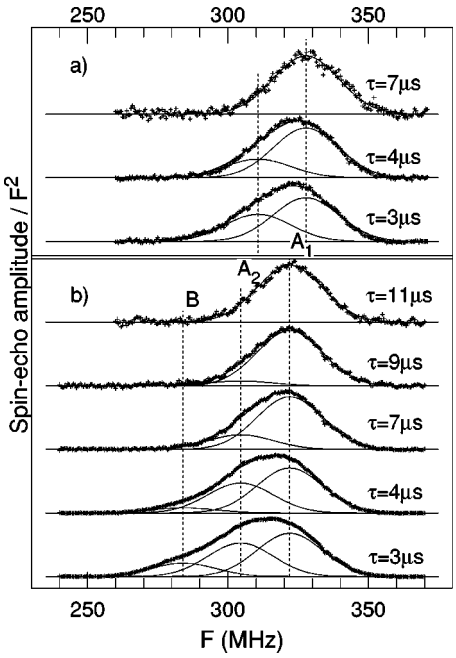

FIG. 3. NMR spectra of ^{55}Mn at $T=155$ K taken at warming (a) and cooling (b) for different values of τ. Spectra for $\tau=4$ and 7 μs (warning) are increased by factor 1.5 and 4.6, respectively. Spectra for $\tau=4$, 7, 9, and 11 μs (cooling) are increased by factor 1.5, 4.3, 8, and 17, respectively. The spectra are decomposed on two (warming) and three (cooling) lines, respectively.

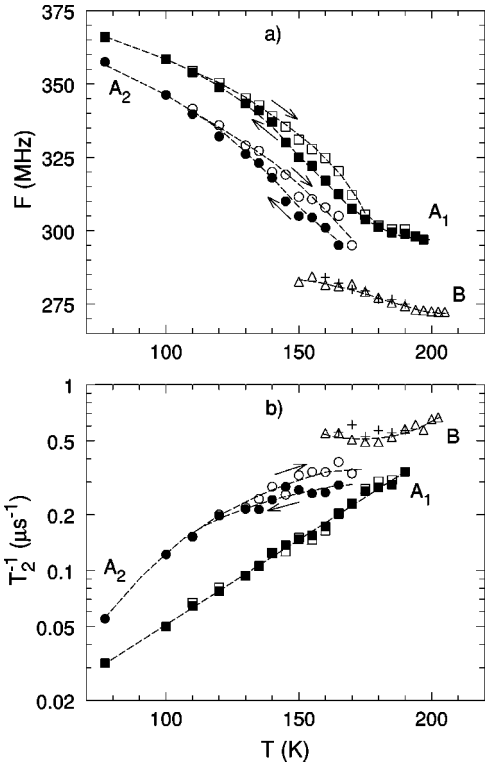

FIG. 4. Temperature dependence the resonance frequency F (a) and spin-spin relaxation rate T_2^{-1} (b) for lines A_1, A_2, and B obtained from a decomposition of the NMR spectra both for cooling (●, filled squares, △) and warming (○,□,×). The dashed curves serve as a guide for eyes only.

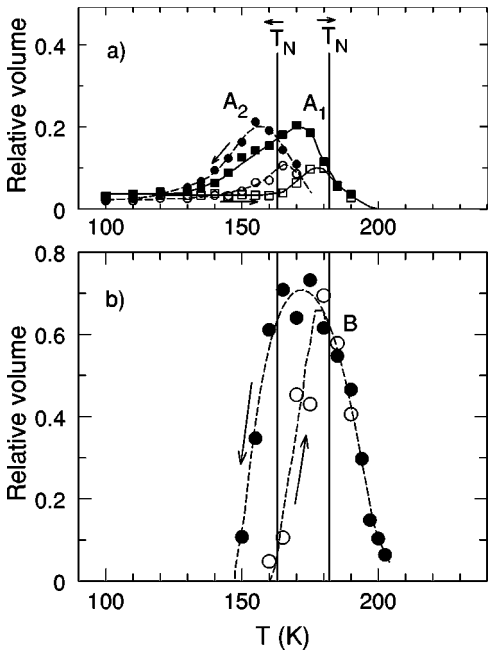

FIG. 5. Temperature dependence of relative volumes of the ferromagnetic phases corresponding to the lines A_1, A_2 (a), and B (b). Filled symbols correspond to cooling while empty symbols correspond to warming. The curves serve as a guide for eyes only.

metalliclike ferromagnetic manganites.[12] The dependence of the relaxation time of line B is almost flat, while the one of line A_2 exhibits a more complex behavior.

In Figs. 5(a) and 5(b) the temperature dependence of relative volumes of the ferromagnetic phases, corresponding to the lines A_1, A_2, B, is displayed. The volumes were obtained from the area under the resonance lines after correcting them for the temperature-dependent enhancement. Besides we took into account the $1/T$ dependence of the spin-echo intensity, which follows from the Curie law for the nuclear magnetic moment.

Inspection of Fig. 5 reveals that above the Néel temperature the prevailing magnetic phase corresponds to the line B and it is therefore to be associated with the bulk ferromagnetism existing between T_N and T_C. In this temperature interval the frequency F_B [Fig. 4(a)], which is proportional to the local electronic magnetic moment, decreases by only $\approx 4\%$ with increasing temperature. In the same temperature interval the volume of the phase B changes dramatically, which points to the phase separation and redistribution of the phase B with a nonferromagnetic phase (antiferromagnetic below T_N and likely paramagnetic for $T \rightarrow T_C$). Comparison of our NMR results with the magnetic and neutron-diffraction data[10] suggests that a fraction of phase B is considerable–at least 50% of the sample volume at the temperature where it attains maximum. Nevertheless below T_C the system remains semiconducting[10] in distinction to ferromagnetic manganites with $\approx 30\%$ concentration of Mn^{4+} ions and similar Curie temperature, which exhibit transition to a metallic state near T_C.[13] This points to a strong tendency of electrons in the present compound to localization and charge ordering. In the phase diagram of the $Pr_{0.5}Ca_{0.5-x}Sr_xMnO_3$ system,[10] the paramagnetic charge ordering temperature decreases from 250 K for $x=0$ to 215 K

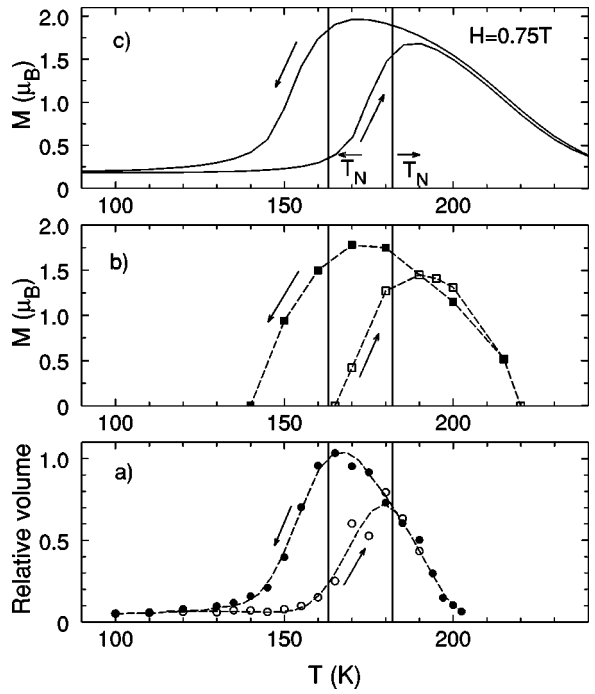

FIG. 6. Temperature dependence of the total volume of the ferromagnetic phases as seen by NMR (a), compared with the magnetic moment determined by neutron diffraction (b, taken from Ref. 10) and magnetization measurement (c).

for $x=0.2$. By extrapolation, a formation of charge-ordered regions within ferromagnetic $Pr_{0.5}Ca_{0.2}Sr_{0.3}MnO_3$ can be expected at ≈ 200 K. Indeed, the occurrence of such regions below $T=200$ K has been evidenced in a direct way by reevaluation of the former neutron-diffraction data supposing a coexistence of two crystallographic phases—the high-temperature quasicubic phase and the charge-ordered tetragonally distorted one.[14] The unusual ferromagnetism of phase *B* is reflected not only in the flat temperature dependence of corresponding NMR frequency but also in the flat dependence of relaxation time T_2, which both differ qualitatively from those observed in the metalliclike manganites with similar T_C.[12,15,16]

In Fig. 6 the total volume of the ferromagnetic phases, as seen by NMR, is shown as function of temperature. In the same figure the temperature dependencies of the magnetic moment, determined by superconducting quantum interference device measurement at 0.75 T and by the neutron-diffraction data,[10] are displayed. The data collected in Fig. 6 demonstrate that the temperature variation of the magnetic moment, observed by magnetic measurements and neutron diffraction, is mainly due to the variation of the volume of the ferromagnetic phases, the variation of the local electronic magnetic moments being relatively small, at least for $T_N < T < T_C$ [Fig. 4(a)]. At low temperatures, the ferromagnetic volume and magnetic moment dependences agree fairly well. At higher temperatures the NMR data suggest faster decrease of the ferromagnetic volume compared to the magnetic measurements. A possible explanation of this difference may be that as *T* approaches T_C, part of the nuclei relaxes too fast to be detected in the present NMR experiment. It should be also noted that as $T \rightarrow T_C$ the NMR determination of the ferromagnetic volume becomes less and less precise.

Perhaps the most intriguing feature of our results is that at the temperature region where the ferromagnetic phase *B* dominates, another FM phase corresponding to the line A_1 appears. This phase persists well below T_N, thus coexisting with the majority antiferromagnetic phase. At about the Néel temperature an additional line A_2 appears in the NMR spectrum and it accompanies the A_1 line in the whole temperature range where the antiferromagnetism exists. Temperature dependences of the resonance frequencies of lines A_1 and A_2 have very similar form, which indicates that both signals originate from the nuclei with physically similar surrounding. The key to understanding the origin of lines A_1 and A_2 should be sought in the data of Fig. 5(a). Below T_N the amplitudes of the A_1 and A_2 lines are comparable, despite their very pronounced (by one order of magnitude) dependence on temperature. This correlation suggests that lines A_1f and A_2 originate from the spatially connected regions having comparable volumes. It is tempting to attribute the two lines to the microscopic ferromagnetic regions and to the boundary between the ferromagnetic regions and the AFM matrix, respectively. Such assignment is further supported by the thermal hysteresis of frequencies for lines A_1 and A_2 [Fig. 4(a)] and also thermal hysteresis of T_2 for line A_2 [Fig. 4(b)]. This hysteresis suggests (see also Ref. 6) nanoscopic rather than mesoscopic FM domains in $Pr_{0.5}Ca_{0.2}Sr_{0.3}MnO_3$.

We note that recent NMR studies on $Pr_{0.5}Sr_{0.5}MnO_3$ in external magnetic field provide additional information on the character of ferromagnetic microdomains in the low temperature AFM phase.[4] There, two FM lines in the NMR spectrum of ^{55}Mn at 1.3 K were observed. Based on the experimentally observed magnetic shift, the first line at 370 MHz was identified with nuclei in the inner part of ferromagnetic domains, while the second line at 290 MHz was ascribed to nuclei at the domain boundaries with the AFM matrix. They are therefore analogs of our lines A_1 and A_2. Similarly to the present study, the intensity ratio of the two lines was found to be close to one. The difference in the frequency of the line A_2, attributed to the FM domain boundaries in both systems, may be understood if we take into account that the antiferromagnetic arrangement in $Pr_{0.5}Sr_{0.5}MnO_3$ is of the A-type, while it is of the CE-type in $Pr_{0.5}Ca_{0.2}Sr_{0.3}MnO_3$. As A_2 corresponds to the boundary between FM and AFM regions, it is to be expected that its frequency depends on the type of the AFM ordering.

The characteristics of lines A_1 and A_2 lead to following conclusions: (i) we are dealing with a very small clusters, the volume and surface area of which are comparable; (ii) the temperature evolution of the phase volume A_1, A_2 in Fig. 5(a) is due to the change in number of clusters rather than in their size. The ferromagnetic signal A_1 appears just at $T=200$ K when the charge ordering starts to develop as stated above. Physically, it can be associated with the ferromagnetic inclusions in the form of very thin slabs or nanoscale clusters inside the charge-ordered domains, which are necessarily linked to defects in the charge order like antiphase boundaries.[3] The appearance of antiferromagnetism at T_N changes the magnetic state in the neighborhood of ferromagnetic regions and their surface layers become in some way coupled to the antiferromagnetically ordered magnetic moments. This coupling gives rise to the additional signal A_2 at about the Néel temperature.

Recently, Dho *et al.*[7] reported a detailed investigation of the temperature dependence ^{55}Mn NMR in $La_{0.5}Ca_{0.5}MnO_3$, which agrees in general with the results presented in this work. In particular, their line I is an analog of line *B* found by us. They were not able, however, to resolve the complexity of the ferromagnetic phase corresponding to the line II (A_1 and A_2 in the present work) as well as the variation of spin-spin relaxation times throughout the NMR spectra. This may originate likely from the difference in samples. On the other hand, it is clear that the precise NMR experiments are required for the A_1,A_2 decomposition.

The NMR measurements on several other manganites containing 50% of Mn^{4+} are in progress. In calcium richer compound $Pr_{0.5}Ca_{0.35}Sr_{0.15}MnO_3$ only the minority ferromagnetic phase (lines A_1 and A_2) was detected in agreement with the absence of the bulk ferromagnetism, as reported by us earlier.[10] Similar NMR spectra, with lines A_1 and A_2 only, were observed also in our sample $La_{0.5}Ca_{0.5}MnO_3$ characterized by negligible net magnetic moment.

In conclusion, the present NMR study demonstrates that the charge ordering in the half-doped manganite $Pr_{0.5}Ca_{0.2}Sr_{0.3}MnO_3$ is accompanied by a separation of antiferromagnetic and specific ferromagnetic phases. The ferromagnetic species, coexisting at low temperatures with the majority CE-type antiferromagnetism, are clearly distinguished from the bulk ferromagnetism which appears above T_N.

This work was supported by the grants 202/99/0413 and 202/00/1601 of Grant Agency of the Czech Republic.

[1] A. Moreo, S. Yunoki, and E. Dagotto, Science **283**, 2034 (1999).
[2] S. Mori, C.H. Chen, and S-W. Cheong, Phys. Rev. Lett. **81**, 3972 (1998).
[3] N. Fukumoto, S. Mori, N. Yamamoto, Y. Moritomo, T. Katsufuji, C.H. Chen, and S-W. Cheong, Phys. Rev. B **60**, 12 963 (1999).
[4] G. Allodi, R. De Renzi, M. Solzi, K. Kamenev, G. Balakrishnan, and M.W. Pieper, Phys. Rev. B **61**, 5924 (2000).
[5] G. Papavassiliou *et al.*, Phys. Rev. B **55**, 15 000 (1997).
[6] G. Allodi, R. De Renzi, F. Licci, and M.W. Pieper, Phys. Rev. Lett. **81**, 4736 (1998).
[7] J. Dho, I. Kim, and S. Lee, Phys. Rev. B **60**, 14 545 (1999).
[8] Y. Yoshinari, P.C. Hammel, J.D. Thompson, and S-W. Cheong, Phys. Rev. B **60**, 9275 (1999).
[9] G. Papavassiliou *et al.*, Phys. Rev. Lett. **84**, 761 (2000).
[10] S. Krupička, M. Maryško, Z. Jirák, and J. Hejtmánek, J. Magn. Magn. Mater. **206**, 45 (1999).
[11] M. Matsuura and H. Yasuoka, J. Phys. Soc. Jpn. **17**, 1147 (1962).
[12] M.M. Savosta, V.A. Borodin, and P. Novák, Phys. Rev. B **59**, 8778 (1999).
[13] H.Y. Hwang, S-W. Cheong, P.G. Radaelli, M. Marezio, and B. Batlogg, Phys. Rev. Lett. **75**, 914 (1995).
[14] Z. Jirák *et al.* (unpublished).
[15] M.M. Savosta, V.A. Borodin, P. Novák, Z. Jirák, J. Hejtmánek, and M. Maryško, Phys. Rev. B **57**, 13 379 (1998).
[16] M.M. Savosta, J. Hejtmánek, Z. Jirák, M. Maryško, P. Novák, Y. Tomioka, and Y. Tokura, Phys. Rev. B **61**, 6896 (2000).